

Increase in the Platinum Group Elements content in road dust from São Paulo city, Brazil, due to exhaust emissions from vehicle catalytic converter, over a 10-year period

Marcos, Hortellani M.A.^a and Jorge, Sarkis J. E. S. ^a*

- 1 *Instituto de Pesquisas Energéticas e Nucleares (IPEN-CNEN), Av. Lineu Prestes, 2242, São*
- 2 *Paulo, SP 05508-000, Cidade Universitária, 05508-000 São Paulo-SP, Brazil*

*e mail: mahortel@ipen.br

<http://orcid.org/0000-0003-3364-0648>

3 **Abstract**

4 Platinum Group Elements (PGEs) are widely used as catalysts in vehicle emission reduction,
5 and road dust is a primary receptor for PGE releases. However, the determination of PGEs in
6 these samples by ICP-MS is affected by matrix interferences, and measurement and sampling
7 uncertainties are often overlooked. This study presents the first PGEs measurements in road
8 dust samples from São Paulo city avenues, including matrix separation and estimation of
9 measurement uncertainty includes analytical and sampling uncertainties. Measurement
10 uncertainties for PGEs ranged from 12.3% to 19.5%, and analytical uncertainty ranged from
11 2.25% to 5.64%. PGEs concentrations: Pt (2.6 - 227 ng g⁻¹), Pd (16.3 - 1875 ng g⁻¹), Rh (2.02
12 - 257 ng g⁻¹). Three methodologies were applied to evaluate the PGEs and other metals
13 contamination in 54 road dust samples (< 100 µm fraction) collected in 2008, 2016 and 2018
14 at 18 sites with high (17 sites) and low (1 site) volumes of traffic. Metal pollution index
15 (MPI), enrichment factor (EF) and statistical analyses. These evaluations suggested that
16 PGEs and Mo contamination were originated from automobile exhaust emissions. Cu and Zn
17 contamination seemed to have been caused by tires and brakes vehicular sources (non-
18 exhaust emissions), but Ni and Pb contamination seemed from non-vehicular sources. Only
19 rare earth elements are mostly associated with crustal source. The changes in PGE ratios
20 stemmed from decreased Pt and increased Pd concentrations. A considerable portion of these
21 metals in road dust is bioaccessible and poses health risks to the population near high-traffic
22 density avenues, through ingestion, dermal contact, and inhalation pathways.

23 **Keywords:** Road dust, Platinum group elements, Metal contamination, Rare earth elements,
24 matrix separation, ICP-MS, enrichment factor.

25

26 1. Introduction

27 São Paulo is the largest City in South America, with a population of 11.45 million in
28 2023 (IBGE-Population, 2023). In October 2008, the city reported 5.5 million vehicles, 7.8
29 million in October 2016 and 8.2 million in September 2018. About 70% of the total used
30 catalytic converters (IBGE-Cities-Brazil, 2023).

31 The use of vehicle catalytic converters to reduce emissions of NO_x, CO and
32 hydrocarbons (HC) to below legislated limits in Brazil started in 1992-1993. But these
33 catalytic converters went into effect in 1996 (Morcelli et al., 2005).

34 Canada, the United States and Japan have used the catalytic converters in car exhaust
35 systems containing Pt, Pd and Rh, since 1976 (Barbante et al., 2001). In the European Union
36 (EU), all new cars registered from January 1st, 1993, have been fitted with catalytic
37 converters to reduce these emissions (Motelica-Heino et al., 2001).

38 The catalysts contribute to the improvement of air quality, but cause a significant
39 increase of environmental contamination. The high temperatures, vibrations, abrasion and
40 attrition bring about the release of PGEs (nanometer size range particles and associations
41 with other metals as part of the coating to which they are connected in the converters) to the
42 environment (Spada et al., 2012; Ravindra et al., 2004; Whiteley & Murray, 2003, 2005).

43 PGE proportions in catalytic converters vary globally and in different years, due to
44 design and fuel differences. Road dusts are considered, the primary receptor for PGEs in
45 urban environments (Spada et al., 2012). It is important to verify the different proportions of
46 PGEs in São Paulo, Brazil, between 2008 and 2018, and comparison with other cities around
47 the world.

48 Studies showed that the Pd is more soluble and bioavailable than Pt and Rh (Jarvis et
49 al., 2001; and Moldovan et al., 2001). Platinum can enter the food chain by accumulation in
50 plants (Verstraete et al., 1998).

51 It also describes, in broad term, that Pt (II), Pt (V) and Pd (II) have been found to be
52 toxic on a cellular level comparable or even exceeding the toxic effects of Cd(II) and e Cr
53 (VI) (Kalavrouziotis & Koukoulakis, 2009). On the other hands, the Rhodium plays no
54 natural biological role and is harmless to humans (Birke et al., 2018).

55 A Daphnia toxicity test, used by (Zimmermann et al., 2017), showed that the PGEs
56 toxicity to Daphnia magna decreased in the order Pd > Pt >> Rh with e.g. LC50(48 h) values
57 of 14 mg/L for Pd, 157 mg/L for Pt and 56,800 mg/L for Rh.

58 PGEs levels in road dust samples from São Paulo city have not been determined yet.
59 However, significant increases in PGE levels were observed in roadside soils from an
60 important road in the State of São Paulo, attributed to catalytic converter exhausts (Morcelli
61 et al., 2005). Additionally, urban soils collected next to seven main avenues with high traffic
62 density in the metropolitan region of São Paulo also demonstrated a relationship between the
63 PGEs and catalytic converter abrasion (Ribeiro et al., 2012).

64 PGEs determination in environmental samples by ICP-MS involves matrix
65 interferences. Correct measurement requires removing interferences through anionic or
66 cationic-exchange resin (Spada et al., 2012), Tellurium coprecipitation (Gomez et al., 2003),
67 or mathematical correction (Moldovan et al., 1999). Ion-exchange removes interferences
68 based on the highly stable anionic chloro-complexes of PGEs, separating matrix elements in
69 stable cationic form or weaker anionic species (Kovacheva & Djingova, 2002). PGEs chloro-
70 complexes are separated by elution on cationic exchangers, retaining other matrix elements
71 (Lesniewska et al., 2006); or selectively retained on anion exchange, subsequently eluted
72 (Hann et al., 2001; and Kanitsar et al., 2003).

73 Mathematical correction, on the other hand, is usually a tedious task since it requires
74 determining and mathematically correcting all interfering species (Moldovan et al., 1999).

75 This study's objective was to investigate, for the first time, PGEs concentrations (Pt,
76 Pd, Rh) in São Paulo city's road dust. A cation exchange resin was used for matrix separation,
77 eliminating isotopic interferences in PGEs, and the other elements were examined without
78 matrix separation. To increase confidence in the results and support informed decision-
79 making regarding metallic pollution, estimations of measurement, analysis, and sampling
80 uncertainties were conducted. The evaluation of metal pollution employed the metal pollution
81 index (MPI), enrichment factor (EF), and statistical analyses to explore the impact of
82 catalytic converters on PGEs and potential sources of other elements in road dust samples
83 across three sampling campaigns.

84 **2. Experimental**

85 2.1. Study area and road dust sampling preparation

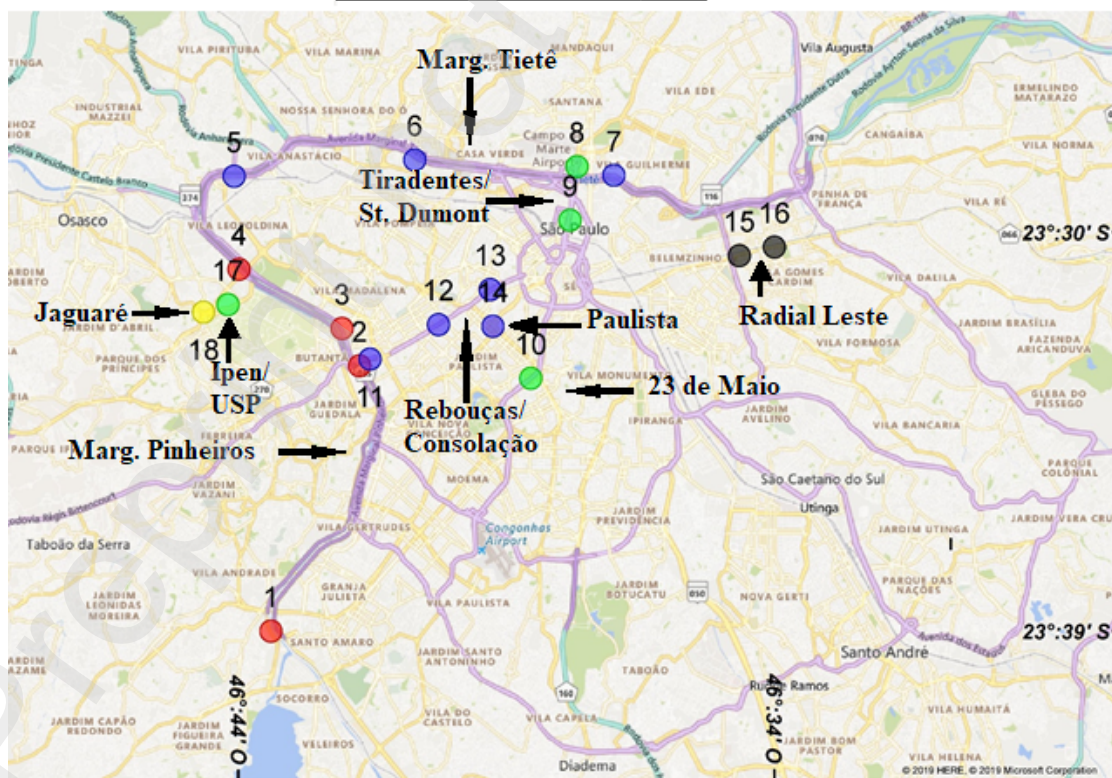
86 A total of 54 road dust samples were collected during three sampling campaigns to
87 investigate variations in the concentration, ratio, and proportion of platinum, palladium, and
88 rhodium. Specifically, 18 samples were collected during the dry winter period in July 2008
89 (1st sampling), another 18 samples were collected during the dry winter period in July 2016
90 (2nd sampling), and the remaining 18 samples were collected during the dry winter period in
91 July 2018 (3rd sampling).

92 Figure 1 shows the locations of the road dust samples selected for this study, which
93 were collected from ten avenues characterized by high traffic density, as well as one location
94 with low traffic volumes known as IPEN-USP Parking, situated in São Paulo city.

95 Among these avenues, the Marginal Pinheiros and Marginal Tietê Avenues are
96 adjacent to the city's two primary rivers, named Pinheiros and Tietê Rivers. These avenues
97 are characterized by a consistently high speed of approximately 90 km/h and no traffic lights.
98 According to a previous study on vehicle flow conducted by Ribeiro et al. (2012), in 1996,
99 Marginal Tietê had an average of 400,000 vehicles per day, while Marginal Pinheiros had

100 around 300,000 vehicles per day. Another significant avenue in São Paulo is the 23 de Maio
101 Avenue, which serves as a connection between the North and South regions of the city, with a
102 steady speed ranging from 50 to 60 km/h and no traffic lights. The remaining avenues
103 included in this study are also key roadways in São Paulo city, featuring traffic lights, high-
104 density stop-and-go traffic patterns, and a speed limit of 50 km/h.

105 The samples were collected within areas measuring approximately 1-2 m² (0.3 x 3 or
106 5m), forming a rectangular grid. A plastic dustpan and brush were used to collect the samples
107 from the gutters of streets and avenues. Subsequently, the samples were transferred to air-
108 tight polyethylene bags for transportation to the laboratory, where they were stored at room
109 temperature.



110
111 **Fig. 1.** Map of the study area and location of the sampling sites.

112 Prior to conducting the analysis, the samples were dried at 80 °C and sieved through
113 meshes with sizes of 2 mm, 1 mm, 150 µm, and 100 µm. The fraction with a diameter smaller
114 than 100 µm was repeatedly quartered until a sample weight of approximately 2 g was
115 obtained. Subsequently, the sample was ground for 10 minutes in a 50 mL centrifuge tube
116 using two plastic balls (Spex) to enhance homogeneity. It is important to note that this
117 fraction, with a diameter smaller than 100 µm, can easily become airborne and inhaled during
118 breathing (Ferreira-Baptista & De Miguel, 2005). This specific fraction was then used to
119 determine the PGEs and other metals.

120 The samples collected in 2008 were archived and reanalyzed alongside the newly
121 collected samples to ensure that any observed increases in PGEs were not due to changes in
122 analytical methods.

123 2.2. Analytical methods

124 2.2.1. Sampling preparation by microwave digestion

125 The samples were digested using a procedure similar to Spada et al.(2012). Digestions
126 of samples were performed in a programmable 1030 -1800 W microwave system (MARS 6,
127 CEM Corp., Matthews, NC) using Xpress 55 mL Teflon vessels rated at 200 °C. Conditions
128 inside the vessels were monitored and controlled in every vessel with an infrared sensor. A
129 known quantity (200 - 400 mg for road dust samples, < 100 µm fraction, and for certified
130 material BCR 723, or 100 mg for certified material SRMs 2556 and 2557) was placed into a
131 Teflon vessel, 8 mL of *acqua regia* was added and left for 5 min and loosely capped. The
132 control points were 200 °C and 300 psig with a ramp time of 20 min. and dwell time of 20
133 min.

134 After cooling, each vessel's content was transferred to a 50-mL centrifuge tube and
135 the volume was increased to 20 mL for samples and BCR, and to 40 mL for SRMs by adding
136 ultrapure water (Milli-Q).

137 After decanting or centrifuging the residues from the vial content, the digestion
138 samples were divided into two parts: one for the determination of Pt, Pd, and Rh, and another
139 for the analysis of the remaining elements (two sub-samples). To determine PGEs, a 10 mL
140 aliquot was evaporated almost to dryness on a hot plate at approximately 80°C in a 50 mL
141 Teflon beaker. The resulting residues were dissolved in 2 mL of concentrated HCl and heated
142 again until almost dry. This treatment was repeated twice more to adequately remove HNO₃.
143 The ultimate residue was dissolved in 10 mL of 0.5M HCl and then subjected to cation
144 exchange elution.

145 2.2.2. Separation on cation-exchange resin

146
147 The interfering species were chemically removed by cation-exchange resin. Before
148 each use, Dowex 50WX8, 200-400 mesh resin was cleaned using a procedure similar to
149 (Spada et al., 2012). Each Poly-Prep column was prepared with 3.5 mL of cleaned resin in
150 0.5M HCl. The resin was first equilibrated with 10 mL of 0.5M HCl and the eluent was
151 collected in a polyethylene tube used as the column background sample preparation. Then,
152 this tube is replaced with a sample tube and 2 mL of sample in 0.5M HCl was added to the
153 column. The eluent was collected at a flow of 0.2 mL min⁻¹. After the samples passed through
154 the column, the resin was rinsed by adding 2 mL 0.5M HCl, collected in the same tube. Then,
155 0.5 ppb of In (internal standard) was added and the final volume was made up to 5 g, and the
156 PGEs concentrations were determined by ICP-MS.

157 2.2.3. Nexion 300D-ICP-MS

158 A Nexion 300D ICP-Mass Instrument (Perkin Elmer) was used to determine PGEs.
159 The isotopes ¹⁹⁴Pt, ¹⁹⁵Pt, ¹⁹⁶Pt, ¹⁰⁴Pd, ¹⁰⁵Pd and ¹⁰³Rh were used to PGEs quantification. The
160 same results were obtained to the multi-isotopic elements Pt and Pd after removing the
161 interfering species.

162 The rare earths elements analyses, Ce, La, Nd, Pr, Sm, Pb and Mo concentration were
163 determined by ICP-MS, after 200 times dilution of sub-samples without ion-exchange
164 separation.

165 A Nexion 300D ICP-MS daily optimization was performed using a $1\mu\text{g L}^{-1}$ NexIon
166 Setup solution (PerkinElmer), consisting of Be, Ce, Fe, In, Li, Mg, Pb, and U in 1% HNO_3 .
167 Formation of oxides ($^{156}\text{CeO}^+ / ^{140}\text{Ce}^+ \leq 0,035$) and doubly charged ions ($^{70}\text{Ce}^{++} / ^{140}\text{Ce} \leq$
168 0.035) were minimized by adjusting the nebulizer gas flow. Auto lens voltage were adjusted
169 to maximize ion transmission based on $^9\text{Be} > 3000$, $^{24}\text{Mg} > 20000$, $^{114}\text{In} > 50000$, and
170 $^{238}\text{U} > 40000$ cps. Under typical operating conditions, sensitivities for ^9Be , ^{24}Mg , ^{115}In , and
171 ^{238}U were approximately 9000, 70000, 70000, and 40100 cps, respectively. Calibration
172 was performed with multi-element standards contained Pt, Pd and Rh and interfering
173 elements (Y, Rb, Sr, Zr, Mo, Cd, Sn, Sb, Pb, and Hf) were also monitored. Cleaning
174 procedures were used for Glass Nebulizer, Cyclonic Spray chamber, Quartz Ball Joint
175 Injector, Nickel cones and Torch when ^{115}In sensitivity was decreased by $\sim 25\%$.

176 2.2.4. Absorption Spectrometer

177 A fast sequential atomic absorption spectrometer Varian, model Spectr-AAS-220Fs
178 was used to determine the Zn, Cu and Ni concentration in the remaining sub-samples without
179 ion-exchange separation, using the flame mode, with deuterium lamp for background
180 corrections. (Hortellani et al., 2013).

181 2.2.5. Reagents and materials

182 All reagents were of analytical grade, (HNO_3 sub boiling and HCl sub boiling). It was
183 used high purity water, of $18\text{ M}\Omega\text{ cm}^{-1}$ resistivity via Synergy System by Millipore
184 Corporation. The PGEs, rare earths elements and Mo stock solution (1000 mg L^{-1}) were
185 acquired (Spex), the Cu, Ni, Pb, Zn stock solution (1000 mg L^{-1}) was acquired (Merck), a
186 cation-exchange resin (Dowex 50WX8 200-400 mesh, Sigma–Aldrich, Saint Louis, MO)

187 were used to chemically separate. The resin was contained in 12 mL Poly-Prep
188 chromatography columns (2 mL bed volume with 10 mL reservoir, Bio-Rad Laboratories
189 Inc., Hercules, CA).

190 ^{115}In was used as an internal standard for all determination to correct instrumental
191 drift or non-spectral interferences because of their low abundance in road dust, similar atomic
192 mass, and broadly similar chemical and physical properties to those of the PGEs.

193 The standard reference materials used consisted of BCR-723 (road dust; European
194 Commission, Joint Research Centre; Institute for reference material and measurement-
195 IRMM), “Used auto Catalyst” (SRM 2556 and SRM 2557), in powder form, NIST, with a
196 certified content of Pt, Pd and Rh, and SRM 2709 San Joaquin Soil –NIST.

197 2.3. Quantification of uncertainties

198 Uncertainty in measurement can be estimated by two components: the uncertainty
199 derived from sampling and the uncertainty derived from the analytical process. The
200 measurement uncertainty (RSD) is given by Eq. (1)

$$201 \quad S_{\text{measurement}}^2 = S_{\text{sampling}}^2 + S_{\text{analytic}}^2 \quad (1)$$

202 2.3.1. Analytical uncertainty

203 The analytical uncertainty was estimated using a modeling approach (Ramsey and
204 Ellison, 2007). The sources of uncertainty were identified, quantified and combined
205 according to Ellison et al. (2002).

206 2.3.2. Sampling uncertainty

207 The sampling uncertainty (S_{sampling}) was calculated by the relative standard derivation,
208 RSD ($S_{\text{measurement}}$), for the steps in the single split design and relative range statistics
209 (Magnusson et al. 2020). To use this single split design, six road dust samples (R1 to R6)
210 were carried out in August 2018, at collection site - 13 (Consolação Avenue). The choice of
211 the point was because it was one of the sites, previously sampled, with highest values of

212 PGEs. Each one of the six samples was considered a sampling target analyzed in duplicate
213 (sample A and sample B) (Tessari-Zampieri et al., 2022) (see Supplementary Information for
214 details). This single split design gives the measurement uncertainty (RSD).

215 Then, the sampling uncertainty S_{sampling} can be calculated using Eq. (2), by rearranging
216 Eq. 1,

$$217 \quad S_{\text{sampling}} = \sqrt{S_{\text{measurement}}^2 - S_{\text{analytic}}^2} \quad (2)$$

218 2.4. Assessment of PGEs contamination

219 Three approaches evaluated the PGEs, earth rare elements and Mo, Zn, Cu, Pb, and Ni
220 results: the Metal Pollution Index (MPI), the Enrichment Factor (EF) and Statistics Analyses.

221 2.4.1. Metal Pollution Index

222 The metal pollution index (MPI) (Eq. (3) (Usero et al., 1996; Okafor & Opuene,
223 2007), was applied to compare the total content of PGEs (Pt, Pd and Rh) between the 18
224 points from the São Paulo city avenues.

$$225 \quad \text{MPI} = (C_{\text{Pt}} \times C_{\text{Pd}} \times C_{\text{Rh}})^{1/3} \quad (3)$$

226 Where:

227 C_{Pt} = concentration value in ppb of the platinum.

228 C_{Pd} = concentration value in ppb of the palladium.

229 C_{Rh} = concentration value in ppb of the rodhium.

230 2.4.2. The Enrichment Factors

231
232 For the estimation of anthropogenic PGEs emissions in road dust samples, it was
233 calculated the enrichment factor (EF) of Pd, Pt and Rh and the other elements with respect to
234 Sm element's crustal concentrations, because Sm is a conservative element (Wedepohl,
235 1995).

236 EF is a useful tool proposed buy Buatmenard & Chesselet (1979) to differentiate the
237 metals source between anthropogenic and crustal concentration.

238 The EF is calculated using Eq. (4):

$$239 \quad EF = \frac{(C_{PGE}/C_{Sm})_{road\ dust}}{(C_{PGE}/C_{Sm})_{crust}} \quad (4)$$

240 Where C_{PGE}/C_{Sm} is the ratio of individual concentration of PGEs or other elements
241 whith Sm.

242 According to Sutherland (2000), $EF < 2$ minimal enrichment (indicative of no
243 pollution), $EF=2$ to 5 is moderate enrichment, $EF = 5$ to 20 is significant enrichment, $EF =20$
244 to 40 is very severe enrichment, and $EF > 40$ is extremely severe enrichment (indicative of
245 extreme pollution).

246 2.4.3. Statistical analyses

247 Statistical differences among the PGEs ratio in the road dust in three samplings were
248 determined with analysis of variance (ANOVA) and considered statistically significant at p-
249 values $<0,05$.

250 The box plot method was also used to better illustrate changes in the PGEs ratio
251 (Pt/Pd, Pt/Rh and Pd/Rh) at three sampling campaigns from 2008, 2016 and 2018, from
252 visual data exploration and outlier detection.

253 The ternary graph was used to compare the varying proportions of PGEs in road dust
254 samples collected during the three sample collections of this study with those from other
255 studies conducted in different countries. The ternary diagram comprises three sides that
256 correspond to Pt, Pd, and Rh concentrations, where the lines of the triangle represent
257 proportions ranging from 0% to 100%.

258 A correlation matrix of all studied variables was performed to identify any existing
259 relationships among the concentrations of the metals studied. Principal Component Analysis
260 (PCA) was applied to examine the various relationships between the variables. The cluster
261 analysis, commonly applied method to environmental evaluation, was used to identify and
262 study the interrelationships among variables and sites exhibiting similar patterns in terms of

263 PGEs concentrations. These statistical analyses were performed using Origin and IBM SPSS
264 Statistics software for Windows.

265 3. Results and Discussion

266 3.1. Optimization of a cation-exchange column for PGEs separation from road dust
267 matrix.

268 In order to confirm the immediate elution of PGEs, the standard solution containing 5
269 $\mu\text{g kg}^{-1}$ of PGEs and interfering elements in similar concentrations as BCR 723 (road dust;
270 certified Rh, Pd and Pt concentrations of 12.8, 6.1 and 81,3 $\mu\text{g kg}^{-1}$ respectively) was
271 prepared and its elution's behavior on Dowex resin was investigated by elution's curves. The
272 simulated solution, 5 mL, was loaded on the columns and was eluted with 11mL 0.5M HCl.
273 The aliquots (1 mL) were collected separately, 0.5 ppb of In (intern standard) was added to
274 each fraction and the PGEs contents were analyzed by ICP-MS.

275 Effective separation of spectral interferences was demonstrated solely by analyzing
276 the Pd concentration using the ^{105}Pd isotope. This interfering specie ($^{90}\text{Zr}^{16}\text{O}^+$), cause
277 interference in ^{106}Pd and $^{92}\text{Mo}^{16}\text{O}^+$ cause interference in ^{108}Pd , (Gomez et al., 2000).
278 However, the Pt isotopes and the monoisotopic Rh showed an effective separation of the
279 interfering isotopes.

280 The elimination of spectral interferences was also monitored by the Mo interference
281 caused in internal standard ^{115}In ($^{115}\text{Mo-O}$ with abundance of 0.03%) which will be detected
282 without saturation effects. Mo was present in high concentration compared to Pd. This value
283 causes saturation of ICP-MS detector that presented a false low intensity to Mo.

284 This experiment aimed to determine the matrix separation efficiency of PGEs using
285 the ICP-MS on cation-exchange resin procedure. For this purpose, 2 mL of the sample
286 solution and 2 mL of 0.5 M HCl were used for rinsing to prevent Zr interference in ^{106}Pd and
287 Mo interference in ^{108}Pd . Additionally, the $^{115}\text{Mo-O}$ interference in ^{115}In was also prevented

288 by using 2mL of sample and 2 mL of 0.5 M HCl for rinsing. Hence, Indium (In) proved to be
289 a suitable internal standard for this procedure.

290 **3.2.** The recovery of the PGEs and other metals using four standard reference material

291 The method validation was performed by analyzing four certified references. Three
292 materials to Pt, Pd, Rh, (SRM 2556 (1), SRM 2557(2) and BCR-723 (3)) and one material to
293 Ce, La, Nd, Pr, Sm, Cu, Zn, Mo, Ni and Pb, (SRM 2709-San Joaquin soil-NIST (4)). In the SI
294 section, a table shows the metals recovery for the four certified reference materials, the
295 detection and determination limits for all metals established agree with INMETRO-2019.

296 The PGEs recovery was $> 80\%$, an indicant of a satisfactory method. Except for
297 elements Pt(3)-75%, Pd(3)-79%, Rh(3)-74%, in BCR-723. These results are in agreement
298 with other studies. Reviewed Literature about the PGEs's contents in the reference material
299 BCR-723 from 2001 to 2006 (Sutherland, 2007); showed Pd concentrations ranging from 4.2
300 to $7.9 \mu\text{g kg}^{-1}$ in the 95% confidence band. In this study it was found Pd concentrations = 4.8
301 $\pm 0.6 \mu\text{g kg}^{-1}$. Another study conducted by Alsenz et al. (2009) reported that the Pd
302 concentration in BCR-723 measurement after mercury co-precipitation by ID-ICP-MS using
303 helium as the collision gas was $4.2\pm 1.4 \mu\text{g kg}^{-1}$, whereas the Pd concentration without helium
304 as collision gas was $7.2\pm 2.5 \mu\text{g kg}^{-1}$. Due to the reduction of molecular interferences by
305 Helium collision, the lower concentration range of $4.2\pm 1.4 \mu\text{g kg}^{-1}$ Pd appears to be more
306 likely, according to the authors' findings.

307 The recoveries of rare earth elements for SRM 2709-San Joaquin soil (4) were: La-
308 76%, Ce-80 %, Nd-79%, Eu-89%, Sm-90% and the non-certified Pr-103%, in comparison to
309 the findings reported by da Silva et al. (2016). Our results agree with da Silva et al.'s study
310 and are in line with the validation data presented by method (USEPA 3051A). It is important
311 to note that Method 3051A, although not fully decomposing the samples, achieved a nearly
312 complete digestion, similar to our study's procedure.

313 The remaining metals recovery for SRM 2709 San Joaquin (4) soil was as follows:
 314 Mo-89%, Cu-104%, Zn-99%, Ni-91%, and Pb-84%. The detection limit for these metals was
 315 obtained based on the mean of determinations of the seven blank preparations (\bar{X}) plus "t"
 316 times the standard deviation determined by these seven blank preparations ($LD = \bar{X} + ts$),
 317 where $t = 3.143$ (the value of "Student's" t for $p = 0.05$ and six degrees of freedom, $n - 1$). The
 318 determination limit was obtained using the equation ($LQ = \bar{X} + 5s$) according to INMETRO-
 319 2019.

320 3.3. Uncertainty

321 The combined uncertainty of analytical results from this study were relatively tiny,
 322 3.7% for Pd, 2.3% for Pt and 5.6% for Rh. The uncertainty associated with samples
 323 preparation ranged from 2 to 8 times higher than analytical uncertainty (2 times for Rh, 4
 324 times for Pd and 8 times for Pt).

325 Table 1 shows the results of estimated uncertainties for PGEs in road dust samples
 326 and comparison between sampling uncertainty (U_{sampling}) in road dust (this work) and the
 327 results of Tessari-Zampieri et al. (2022) that determined PGEs in the fractions deposited on
 328 leaves of plants.

329 Table 1: Values of Uncertainties associated with the PGEs determinations in road dust (this
 330 study) and comparative values of U_{sampling} in road dust whit U_{sampling} in tree Branches (Tessari-
 331 Zampieri et al., 2022).

PGE	u_{analysis} combined standartb $u\%$	$u_{\text{measurement}}$ RSD%	$*U_{\text{measurement}}$	u_{sampling}	$*U_{\text{sampling}}$ This study Road dust	$*U_{\text{sampling}}$ tree branches (Tessari- Zampieri et al., 2022)
Pd	3.7	16.9	34	16.5	33	66
Pt	2.3	19.5	39	19.4	39	48
Rh	5.6	12.3	25	10.9	22	54

332 *The expanded uncertainty (U) was obtained multiplying the measurement ($u_{\text{measurement}}$) and sampling
 333 uncertainty (u_{sampling}) by 2 for a level of confidence of approximately 95 %

335 3.4. PGEs and other metals results

336 In the three sampling campaigns conducted in 2008, 2016, and 2018, concentrations
337 of Pt, Pd, and Rh ranged from 2.6 to 227 ng g⁻¹, 16.3 to 1875 ng g⁻¹, and 2.0 to 257 ng g⁻¹,
338 respectively. The mean Pt/Pd ratios were 0.29, 0.14, and 0.10, for 2008, 2016, and 2018,
339 respectively. These results for 54 samples are present in Supplementary Information Section
340 and suggest a gradual increase in the levels of palladium (Pd) in automotive catalysts over a
341 10-year period.

342 The concentrations of various metals, Mo, Ni, Pb, Cu, Zn, and rare earth elements also
343 were determined and are present in Supplementary Information Section. Among these
344 elements, only the rare earth elements appear to have originated primarily from crustal
345 sources.

346 Thus, the ratios of lanthanides observed in the road dust samples from São Paulo city
347 indicate a predominantly "natural" origin. The median values for the ratios of La/Ce, La/Pr,
348 La/Nd, and La/Sm in this study were 0.5, 4.6, 1.26, and 7.5, respectively. These values
349 closely resemble those found in the continental crust (0.5, 4.89, 1.28, and 6.9, respectively,
350 according to (Wedepohl, 1995).

351 **3.5. Assessment of the increase in Pd concentration**

352 The recent increase in palladium (Pd) concentrations in automotive catalysts aligns
353 with findings from two relevant studies. CETESB (2019) presented emissions data from 2006
354 to 2019, indicating a decreasing trend in pollutant emissions. Despite this reduction, air
355 quality in major cities remains compromised, with elevated levels of ozone and particulate
356 matter (PM) that pose risks to public health. Additionally, the rise in carbon dioxide
357 emissions, primarily driven by the growing urban vehicle fleet, has contributed to global
358 climate change. In the context of human health, Wiseman et al. (2018) investigated the
359 bioaccessibility of platinum group elements (PGEs) in road dust samples using a simulated

360 lung fluid. Their results revealed that platinum exhibited the highest geometric %
361 bioaccessibility (16%), followed by rhodium (14%), and palladium (3.4%).

362 Earlier research conducted by Moldovan et al. (2001) and Jarvis et al. (2001) has
363 shown that palladium (Pd) is more soluble and bioavailable than platinum (Pt) and rhodium
364 (Rh). Additionally, Zimmermann et al. (2017) discovered that the toxicity of Pd to *Daphnia*
365 magna was roughly 11 times higher than that of Pt. These findings indicate that higher levels
366 of Pd could present a greater risk to the environment.

367 **3.6. Comparison with other studies**

368
369 Palladium (Pd) concentrations in road dust samples have increased in the last 20
370 years, as seen in Table 2. In the 15 studies that have been examined, only the initial two
371 studies conducted in Sweden 1998 by (Motelica-Heino et al., 2001) and Hawaii (2002) by
372 (Sutherland et al., 2008), followed by a subsequent 2012 study conducted by Spada et al.
373 (2012) on street dust samples from Houston, Texas, USA, have demonstrated Platinum (Pt)
374 concentrations surpassing those of Palladium (Pd), indicated by a Pt/Pd ratio exceeding 1.
375 Notably, the first study based on road dust samples collected in 1998 by (Motelica-Heino et al.,
376 2001) exhibited a Pt/Pd ratio of 2.5 and a Rhodium (Rh) proportion of 25%, signifying
377 characteristics consistent with the early catalysts employed in the automobile industry. The
378 remaining studies, including the present investigation, exhibited Rh proportions ranging from
379 6% to 13%. Pt enrichment and Pd depletion were partially attributed to the relative
380 predominance of diesel vehicles in Europe (Spada et.al. 2012)

381 The road dust samples collected in São Paulo in 2008 (fraction <100 µm) exhibited an
382 average Pt/Pd ratio of 0.3, a value consistent with one of three prominent cities in the Pearl
383 River Delta region of China, Guangzhou, where ten samples collected in 2008 exhibited a
384 Pt/Pd ratio of 0.2 (QI et al., 2011) (Table 2). A similar Pt/Pd ratio of 0.3 was observed in a
385 road dust sample (fraction <100 µm) obtained from Taiwan in 2012 (HSU et al., 2013).

386 However, a notable decrease in the average Pt/Pd ratio to 0.1 was observed in the road dust
387 samples from São Paulo in 2016 and 2018. Notably, these results are consistent with a
388 previous study conducted in Taiwan in 2012, where a sample exhibited a Pt/Pd ratio of 0.1
389 (Hsu et al., 2013). (Table 2), indicates a lower Pt content compared to the levels observed in
390 2008. Several factors can contribute to variations in Platinum Group Elements (PGEs)
391 concentrations in road dust across different countries, including geographic, topographic, and
392 climatic disparities, traffic patterns, vehicle characteristics, maintenance practices, catalytic
393 converter designs, prevailing environmental regulations, and fuel types.

394 Table 2 also presents the Pt/Pd ratio (1.0) with consistent proportions of Pt and Pd
395 (both at 45%) among the total Platinum Group Elements (PGEs) found in road dust samples
396 collected in Perth, Australia, in 2002, by Whiteley and Murray (2003). Furthermore, other
397 studies conducted in various locations provide additional Pt/Pd ratios ranging from 0.5 to 0.7:
398 Guangzhou, China, in 2009 (0.7) by Zhong et al. (2012); Beijing, China, in 2010 (0.5) by
399 Gao et al. (2012); Seoul and Newcastle, England, Europe, in 2014 (0.5) by Okorie et al.
400 (2015); Houston, Texas, USA, in tunnel dust in 2012 (0.7) by (Spada et.al. 2012); and
401 Toronto, Canada, in the inhalable fraction of road dust in 2015 (0.6) by Wiseman (2018).
402 These findings indicate a recent increase in the usage of Pd compared to Pt in automotive
403 catalysts.

404 **Table 2.** Comparative values of Pt, Pd and Rh in road dust in relation to this study

References	Sample Year	Sample location (samples numbers, fraction examined (μm))	PGEs ($\mu\text{g kg}^{-1}$)			Pt/Pd	% Rh
			Pt	Pd	Rh		
(Motelica-Heino et al., 2001)	1998	(Goteborg, Sweden (n=1, < 63))	^(c) 195 \pm 17	^(c) 68 \pm 5	^(c) 90 \pm 11	2.9	25
(Sutherland et al., 2008)	2002	Honolulu, Hawaii (n=12, < 63)	^(b) 4.1 – 173.8 ^(c) 51.8 \pm 53	^(b) 1.7- 101 ^(c) 29 \pm 32	^(b) 0.24–15.8 ^(c) 5.2 \pm 5.1	1.8	6
(Whiteley & Murray, 2003)	2002	Perth, Australia (n=9, < 63)	^(b) 53.8 – 419.4 ^(a) 200	^(b) 58.2 – 440.5 ^(a) 199	^(b) 8.8 – 91.4 ^(a) 41	1.0	9
(Qi et al., 2011)	2007-2008	Shenzhen (n=13, <150)	^(a) 111.8	^(a) 154.0	^(a) 29.6	0.7	10
		Guangzhou (n=10, < 150)	^(a) 23.4	^(a) 97.8	^(a) 6.9	0.2	5
		Hong Kong (n=12, <150)	^(a) 57	^(a) 75	^(a) 9.4	0.8	7
(Zhong et al., 2012)	2009	Guangzhou, China (n=35, <63)	^(a) 68	^(a) 93	^(a) 24	0.7	7
(Gao et al., 2012)	2010	Beijing, China(n=158, <63)	^(b) (9.4-182.9) ^(a) 56.2	^(b) (17.4-458.8) ^(a) 112.6	^(b) (4.0 – 68.0) ^(a) 19.9	0.5	11
(Spada et al., 2012)	2012-streets	Houston, Texas (n=4, < 63)	^(b) 35 – 131	^(b) 10 – 88	^(b) 6 – 8	1.5 - 3	----
	2012-tunnel		^(c) 529 \pm 130	^(c) 770 \pm 208	^(c) 152 \pm 52	0.7	11
(Hsu et al., 2013)	2012-AM-1	Taiwan (n=2, < 100)	^(a) 148	^(a) 485	^(a) 32.2	0.3	5
	2012-AM-2		^(a) 30.2	^(a) 381	^(a) 21.1	0.1	5
(Wiseman et al., 2018)	2015	Toronto, Canada (n=64, <10)	^(a) 31	^(a) 85	^(a) 11	0.6	9
(Okorie et al., 2015)	2014	New Castle, United Kingdom (n=9, < 250 μm)	^(a) 36	^(a) 80	^(a) 18	0.5	13
This study	2008	São Paulo, Brazil (n=18, < 100)	^(b) 5.5 – 171 ^(a) 79	^(b) 16.3 – 1034 ^(a) 268	^(b) 2.4 – 85 ^(a) 39	0.3 ^(a)	10
This study	2016	São Paulo, Brazil (n=18, < 100)	^(b) 2.6 – 191 ^(a) 69	^(b) 22.5 – 1832 ^(a) 505	^(b) 2.0 – 192 ^(a) 59	0.18 ^(a)	9
This study	2018	São Paulo, Brazil (n=18, < 100)	^(b) 2.8 – 227 ^(a) 64	^(b) 2..3 – 1875 ^(a) 640	^(b) 2.8 – 257 ^(a) 73	0.10 ^(a)	9

405 (means^(a), range^(b) and means \pm SD^(c))

3.7. Three approaches are used to interpret the results.

3.7.1. Metal pollution index

The Metal Pollution Index (MPI), as defined in equation 3, was used to assess the presence of PGEs contamination in road dust over a specific time period. The results revealed a gradual escalation in PGEs contamination, with the mean MPI values increasing from 90 in 2008 to 123 in 2016, and further to 143 in 2018. The most severe pollution levels ($MPI > 300$) were observed at point 12 in both the 2016 and 2018 samples, as well as at points 13 and 14 in 2016. These specific locations are situated near heavily congested avenues with stop-and-go traffic, traffic lights, and a speed limit of 50 km/h.

In the 2018 sample collection, several other locations also displayed elevated PGE pollution indices ($MPI > 200$), namely points 9, 10, 16, and 18. These locations also experience high levels of traffic. In contrast, the lowest MPI (6, 5, and 6 in 2008, 2016, and 2018, respectively) was recorded at point 17 (Ipen/USP-Parking), which is characterized by low traffic volumes. Interestingly, point P-12 exhibited a total PGE concentration (MPI) that was approximately 60 times higher than that of point P-17 (Ipen/USP-Parking). Despite having the lowest MPI, indicating relatively low PGE contamination, point P-17 is still influenced by the same anthropogenic vehicular sources as the other sampling locations.

These results align with the results reported by Wichmann et al. (2007), which identified higher concentrations of PGEs in central and busy streets with stop-and-go traffic in Germany. The concentrations were approximately 2.2 times higher compared to the central lanes of avenues where vehicles maintained a constant speed of 50 km/h.

It was also observed by Merget and Rosner (2001) that automotive catalysts emit Pt under various operating conditions, as studied using a dynamometer in different scenarios. In urban areas, where vehicle speeds are lower and there is stop-and-go traffic, Pt emissions were measured at 60 ng km^{-1} , whereas at a constant speed of 80 km h^{-1} , emissions were reduced to 20 ng km^{-1} .

3.7.2. The Enrichment factor EF

The enrichment factor (EF) for individual PGEs (Pt, Pd, or Rh) and other metals present in road dust was determined in relation to the crustal concentration of samarium (Sm), as described by equation 4. In this study, samarium (Sm) was selected as the reference element due to its origin being indistinguishable from

433 the upper continental crust, and it exhibited a 90% recovery rate for certified reference materials. The
434 reference values used for the Earth's crust (WEDEPOHL, 1995) were as follows: 5.3 $\mu\text{g g}^{-1}$ for Sm,
435 0.4 ng g^{-1} for Pt, 0.4 ng g^{-1} for Pd, and 0.06 ng g^{-1} for Rh.

436 Fig. 2a presents average EF for Pt and shows stability, with a small decrease from 142 in 2008 to 128
437 in 2016, followed by a slight increase to 148 in 2018. On the other hand, the average EF values for both Pd
438 (509, 942 and 1507) and Rh (487, 729 and 1119) showed an increase between 2008, 2016 and 2018,
439 respectively. These results indicate a consistent rise in Pd and Rh contents since 2008, likely attributed to the
440 increasing number of vehicles and changes in the proportion of PGEs used in automotive catalysts.

441 In contrast, Point 17 (IPEN parking) consistently exhibited the lowest EF levels throughout the three
442 sampling campaigns. However, despite being a relatively lower EF compared to other sites, there was a very
443 high enrichment for Pd (19, 51 and 30), a significant enrichment for Pt (7, 6 and 4) and a very high
444 enrichment for Rh (19, 31 and 25) between 2008, 2016 and 2018, respectively. These values exceed $\text{EF} > 2$,
445 which indicates a low pollution or non-polluted status. All the samples sites, except for site P-17, showed an
446 EF much higher than 40 for PGEs, indicating an extremely high enrichment of PGEs, based on the
447 categories proposed by SUTHERLAND (2000).

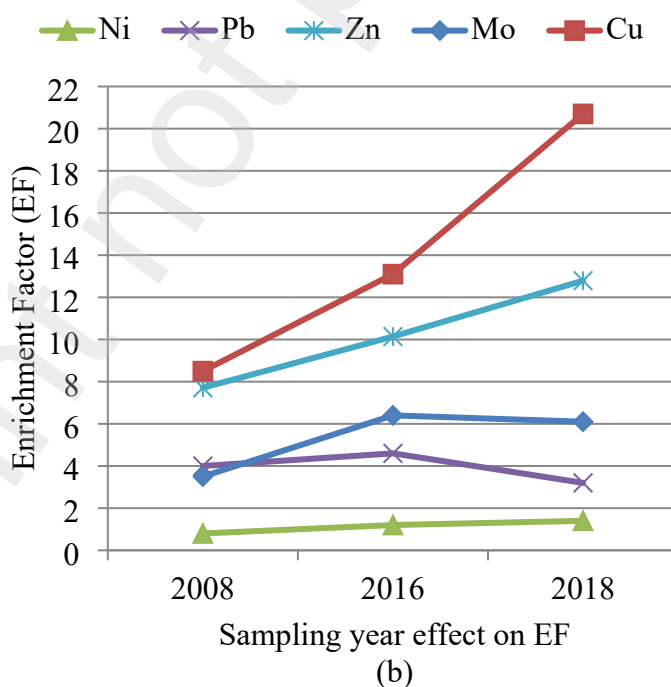
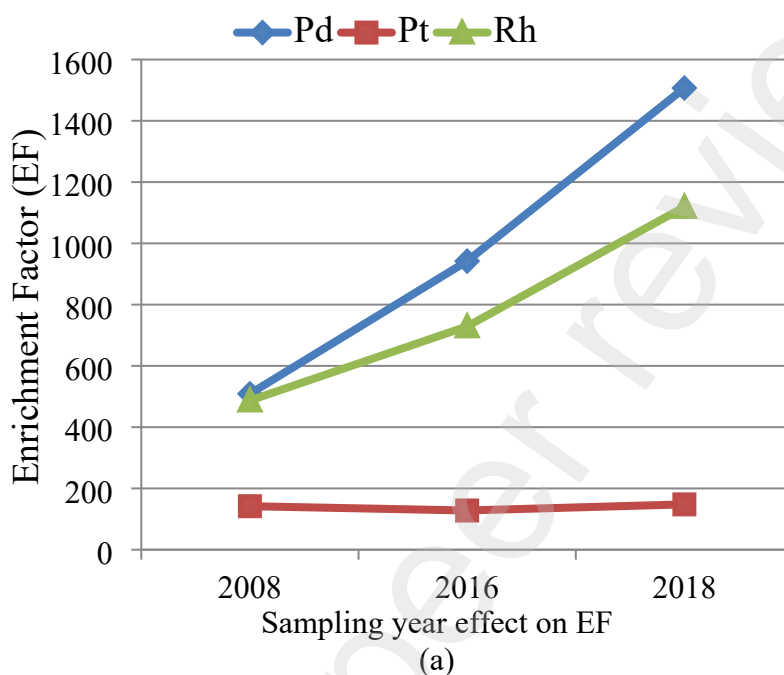
448 In general terms, the most critical areas concerning PGEs accumulation ($\text{EF} > 40$) are sites P-12, P-13,
449 P-14 and P-10. These locations are also situated near heavily congested avenues with stop-and-go traffic,
450 traffic lights, and a speed limit of 50 km h^{-1} .

451 Fig. 2b shows an increase of Cu, Zn and Mo EF in road dusts sampling 2008, 2016 and 2018, likely
452 attributed to the increasing number of vehicles, suggesting their vehicular origins.

453 On the other hand, Pb and Ni do not seem to be associated with contamination due to vehicular
454 origins. Since the average EFs did not increase with the increase in the vehicle fleet between 2008 to 2018.
455 Ni showed $\text{EF} < 2$ (mean) with deficiency to minimal enrichment for the three sampling campaigns 2008,
456 2016 and 2018. Only 4 of 54 samples showed $\text{EF} 2\text{--}5$ indicative of a moderate enrichment.

457 Pb concentration in 20% of total of 54 samples presented $\text{EF} < 2$ (Deficiency to minimal
458 enrichment), 60% presented $\text{EF} 2 - 5$ (moderate enrichment) and 20% presented $\text{EF} 5- 20$ (Significant
459 enrichment). Part of Pb contamination in tunnel dust analyzed by Nory et al. (2021) was attributed to the

460 burning of fossil fuels. The addition of Pb to gasoline in Brazil was only done until 1989. However, the Pb
 461 emitted by leaded gasoline can still be found in the urban environment due to resuspension from the
 462 superficial layer of soil (Lima et al., 2023). The average residence time of Pb ranges from 170 to 250 years
 463 (Klaminder et al., 2006). EF results for 54 samples and all metals are present in Supplementary Information
 464 Section.



466 **Fig. 2.** Enrichment factors in road dust samples for PGEs (Fig.2a) and Cu, Mo, Ni, Pb and Zn (Fig.2b) using
 467 Sm as the crustal source reference.
 468
 469

470 Fig. 3d shows a box plot with the Pt, Pd, and Rh EF from all 54 samples in three sampling
471 campaigns, where an increase in Pd and Rh contamination, but stabilization in Pt contamination, was
472 observed.

473 3.7.3. Statistical analyses

474 Variations in the PGEs ratio among three samples campaigns, 2008, 2016, 2018, were determined with
475 ANOVA and considered statistically significant ($p < 0.05$), suggesting that annual variations may contribute
476 to change the ratio of PGEs. However, changes of PGEs ratios for all site in the same year, also were
477 compared using ANOVA and considered statistically insignificant ($p > 0.05$), suggesting that PGEs ratio in
478 these road dust samples did not change significantly in the same year.

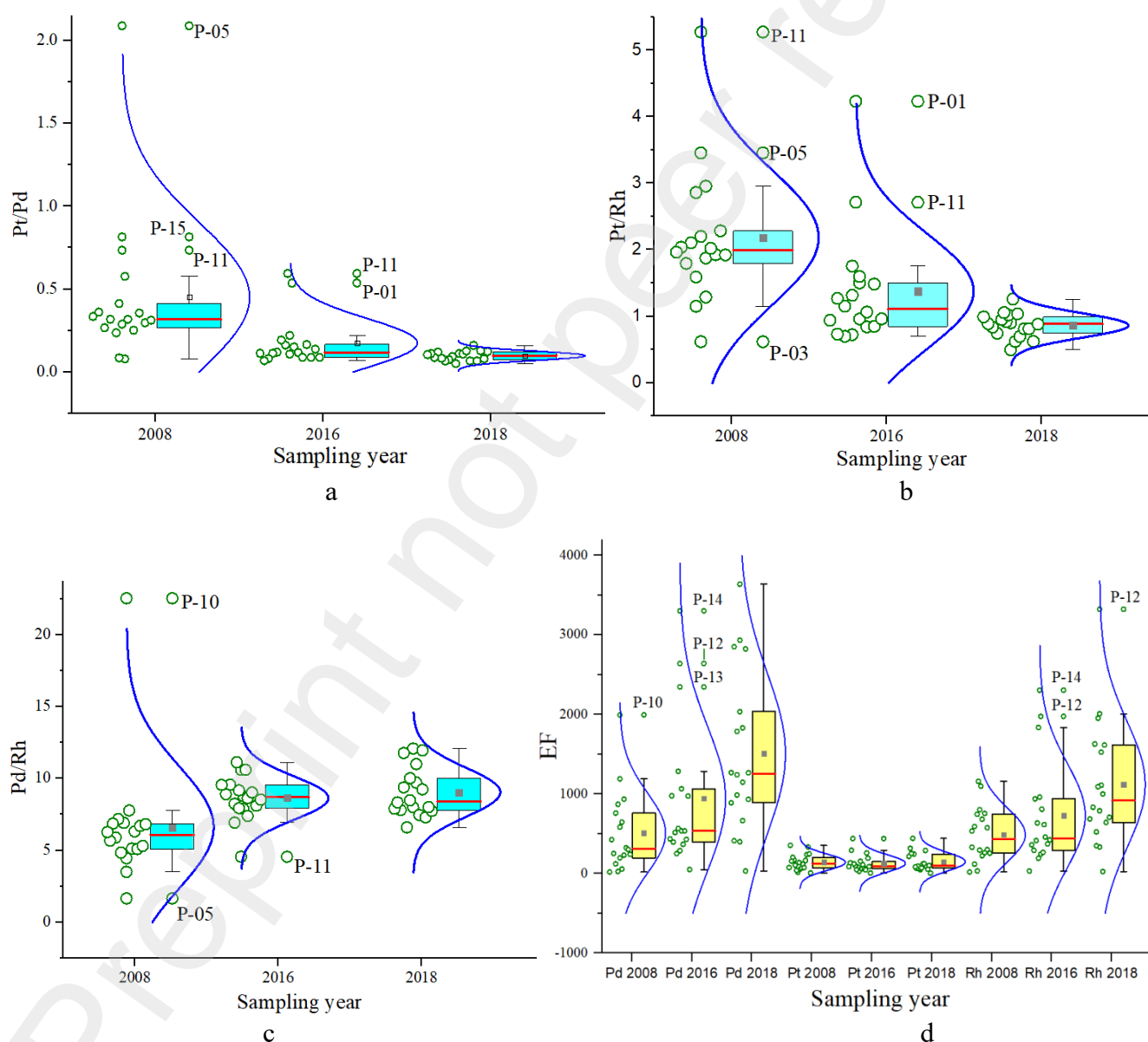
479 3.7.3.1. Box plot from PGEs ratio at the three sampling campaigns.

480 The box plot method was used to better illustrate changes in the PGEs ratio in road dust samples at three
481 sampling campaigns (Figure 3). The box plot uses the median, the approximate quartiles, and the lowest and
482 highest data points to convey the level, spread, symmetry of a distribution of data values and a normal
483 distribution curve. The changes of PGEs concentration ratios (Pt/Pd, Pt/Rh and Pd/Rh) have been evident in
484 the last years.

485 Fig. 3a illustrates a decline in Pt concentration and a rise in Pd concentration over the years 2008,
486 2016, and 2018. The median Pt/Pd ratio for the 2008 samples is significantly higher compared to that of
487 2016 and 2018. A wider normal distribution curve indicates increased data dispersion, leading to a wider
488 range of values and higher variability. Additionally, outlier values were observed for Pt/Pd in samples P-03,
489 P-05, P-10, P-11, and P-15 during the 2008 sampling campaign, and in samples P-01 and P-11 during the
490 2016 sampling campaign. However, the data from 2018 reveal a smaller amplitude, and the normal
491 distribution curve remains relatively narrow, concentrated around the median in the observed values. This
492 signifies a reduced range of values and consistent data distribution. In Such cases, without outlier values, it
493 indicates a stabilization of the Pt/Pd ratios. These findings validate the ongoing shift in automotive catalysts
494 over the past 20 years, which involves an increase in Pd concentrations and a decrease in Pt levels.

495 Fig. 3b shows a decrease in the Pt/Rh ratio from 2008 to 2016 and 2018. This can be attributed to the
 496 limited effectiveness of Pt/Rh in reducing aldehyde emissions from Brazilian ethanol-fueled vehicles
 497 (Miguel and de Andrade, 1990). Additionally, a wider normal distribution curve and a presence of outlier's
 498 values and a narrow normal distribution curve were detected in 2008 and 2016. However, no outlier's values
 499 and a relative narrow normal distribution curve were detected in 2018, indicating that the ratios have
 500 reached a state of stability.

501 Fig. 3c shows an increase in the Pd/Rh ratio, indicating a rise in both Pd and Rh concentrations from
 502 2008 to 2016. However, from 2016 to 2018, the ratio remained relatively constant, accompanied by a
 503 relatively narrow normal distribution curve.



504
505
506

507
508
509

510 **Fig. 3.** Box plot of PGEs ratios Pt/Pd (a), Pt/Rh (b), Pd/Rh (c) and EF (d) for 54 road dust samples collected
 511 in three sampling campaigns. A solid red line within the box indicates a median value. Horizontal lines

512 in the boxes represents 25, 50(median) and 75% of values; error bars indicate 5 and 105% of these
513 values. Green open circle on the left side of the box represents the 18 samples of each collection. Green
514 open circle above or below the box represents outlying points and a normal distribution curve is
515 indicated with blue vertical lines.

517 3.7.3.2. Application of ternary diagram in the PGEs results

518 Ternary diagrams, Fig. 4, display PGEs proportions (Pd, Pt, and Rh) in the three sampling campaigns
519 (this study), compared with 2 São Paulo soil samples, three certified materials and road dust samples from
520 another country.

521 The total sum of PGEs concentrations is represented as 100% in the ternary representation. Fig. 4a
522 indicates a higher point dispersion in the 2008 sampling collection (red color), suggesting a transition in
523 PGEs concentrations in catalysts. Considering the average age of São Paulo vehicles is 9.7 years, potential
524 scenarios encompass older cars with higher Pt content and newer ones with reduced Pt.

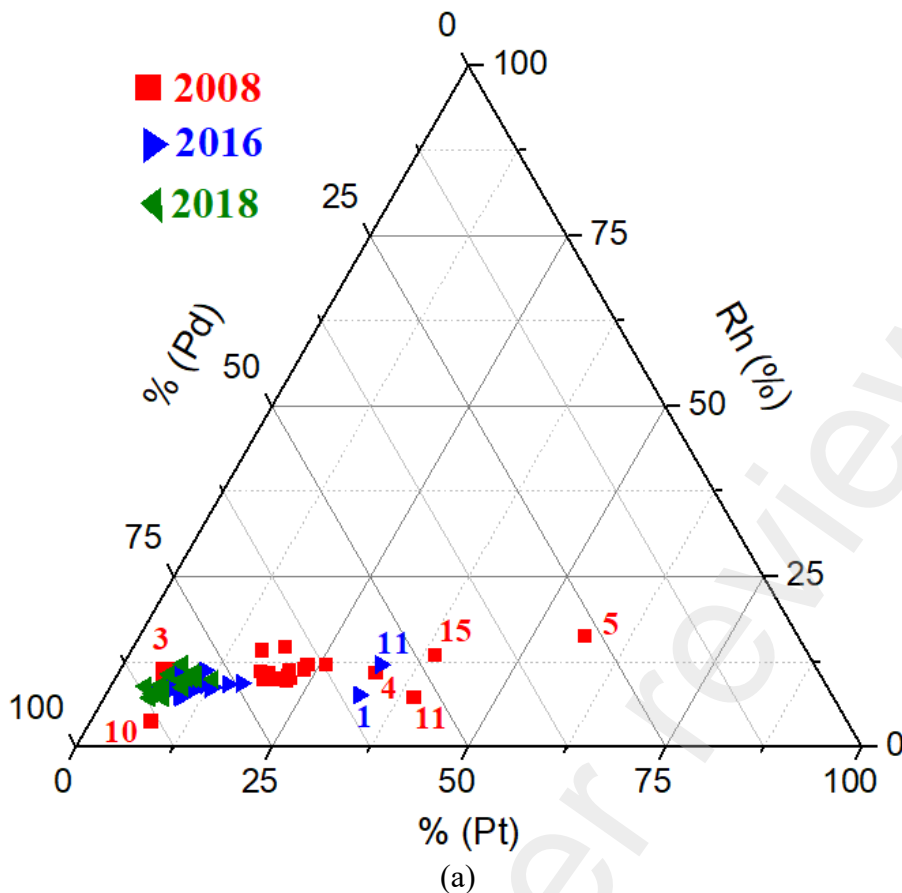
525 Samples from 2016 also in Fig. 4(a), (blue color) had only 2 points (11 and 1) close to 2008 samples.
526 Furthermore, it's evident that the 2018 samples (green color) are closely grouped, suggesting stabilization in
527 the reduction of Pt and an increase in Pd concentration. Points have little dispersion, close to most 2016
528 samples. These data align with automotive catalyst composition changes, reducing Pt content from 2000
529 (Birke et al., 2018).

530 Fig. 4b shows the mean proportions of Pt, Pd, and Rh in road dust samples from 2008, 2016, and
531 2018, along with three certified reference materials and soil samples from São Paulo (Morcelli et al., 2005;
532 Ribeiro et al., 2012). The 2008 road dust samples showed a 7-fold increase in PGEs concentrations
533 compared to 2002 soil samples. However, in 2008, there was a 3-fold increase in Pt and Pd, and a 6-fold
534 increase in Rh compared to 2008 soil samples. PGEs proportions in road dusts and soils align with known
535 catalytic converter composition, indicating that the PGEs remain associated during mobilization and
536 transport (Whiteley, 2005).

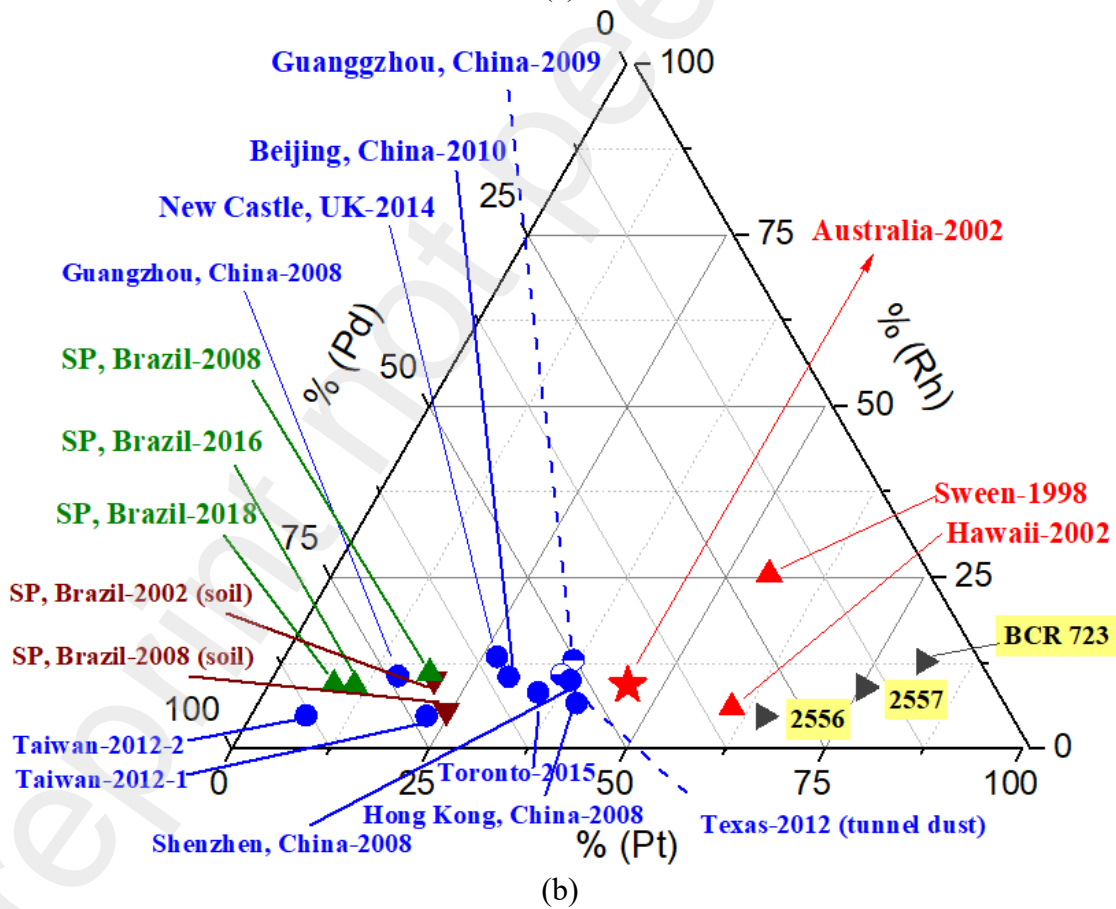
537 Figure 4b also compares the mean proportions of Pt, Pd, and Rh in road dust samples from various
538 countries. Cities with the highest Pt/Pd ratio, such as Sweden 1998 (Motelica-Heino et al., 2001) and Hawaii
539 2002 (Sutherland et al., 2008), are positioned to the right of Perth, Australia 2002 (Whiteley & Murray,
540 2003) on the Pt and Pd axis (with a Pt/Pd ratio of 1), represented by a red star. Conversely, all other cities

541 positioned to the left exhibited a higher concentration of Pd compared to Pt. São Paulo's 2018 samples
542 resemble Taiwan's 2012 sample (HSU et al., 2013). Various fuel types (diesel, gasoline, and alcohol)
543 influence the PGEs compositions of automotive catalytic converters. In Europe, the predominance of diesel
544 vehicles results in relative Pt enrichment and Pd depletion (Spada et al., 2012). Conversely, in Brazil,
545 alcohol use leads to Pt depletion due to less effective Pt/Rh utilization, while Pd increases when used as
546 Pd/Mo, demonstrating better efficiency (Miguel and de Andrade, 1990; Baldanza et al., 2000).

547



548
549



550
551
552
553
554
555
556

Fig. 4: Ternary diagram comparing the relative proportion of Pd, Pt and Rh in the 54 road dust samples collected in three sampling campaigns (this study) Fig. 4a. and mean of Pd, Pt, and Rh relative proportion for 2008, 2016 and 2018 samples compared to mean of soil samples collected in 2002 from other studies by (Morcelli et al., 2005) and in 2008 by (Ribeiro et al., 2012) in São Paulo city, three certified reference materials (SRM 2556, SRM 2557, and BCR723), and to other studies in Fig. 4b.

3.7.3.3. Correlation matrix

A Pearson correlation analysis was performed to assess the strength of relationships between the analyzed metals. The metals Pd, Rh, Pt, and Mo showed a strong correlation ($p < 0.01$), indicating a common origin, likely from vehicle emissions. Cu and Zn also had a significant correlation ($p < 0.01$) with Pt, Pd, Rh, and Mo, suggesting a similar source from vehicles. The rare earth elements (Ce, La, Nd, Pr, Eu, and Sm) exhibited a significant correlation ($p < 0.01$) among themselves, implying erosion of crustal materials as their source. However, neither Ni nor Pb showed a significant correlation with any other elements. This analysis did not identify distinct groups of metals with similar behavior.

3.7.3.4. Cluster and PCA Analysis

Cluster analysis groups similar elements and samples using a dendrogram, examining distances between datasets to summarize similarity of variables (PGEs, Mo, Cu, Zn, Ni, Pb, and rare earth elements). Figure 5 shows the dendrogram with horizontal links for elements/sites and numbers indicating similarity levels (0 to 25). Sites clustered into two groups (G1 and G2) based on maximum dissimilarity among PGEs, Mo, Cu, Zn, Ni, Pb, and rare earth elements (Fig. 5a) and PGEs' content in road dust samples (Fig. 5c).

Fig. 5a shows a group G1 with the PGEs Pd, Rh, Mo and Pt grouping by their similarity, Pd, Rh and Mo have been a significant increase in their concentration over this ten-year period, and Pt had a little dissimilarity with a small decrease in its concentration in that same period, group G1-A-1. These small dissimilarities between the PGEs were caused by a decrease in the concentration of Pt (platinum) due to Pt/Rh (platinum/rhodium) exhibiting low efficiency when used with alcohol fuel, and an increase in the concentration of Pd (palladium) used as Pd/Mo (palladium/molybdenum) with better efficiency (Miguel and de Andrade, 1990). Cu and Zn contamination, (Group G1-A-2) seemed to have been caused by tires and brakes from the same vehicular sources (non-exhaust emissions).

The Group 1B with the Pb and Ni was isolated from the group of PGEs because Ni presented moderate enrichment in 7% of the 54 samples and Pb presented 60% of the samples with a moderate contamination and spread by São Paulo and 20% with a significant enrichment. These observations suggested that the Pb has a moderate contamination and spread by São Paulo, although Pb and Ni that presented some sites with significant enrichment, but not in the same sites most impacted with very high

585 enrichment and extremely high enrichment as for the PGEs. While, the group G2 (Ce, La, Nd, Pr and Sm)
586 was separated from the group G1 by the maximum dissimilarity. This G2 presented concentration seemed to
587 be associated with erosion of crustal material or natural weathering processes.

588 Fig. 5b displays the results of the principal component analysis (PCA), where the 14 variables are
589 represented by three new variables called Main Components (PC). These PCs account for 74.9% of the total
590 variance in the original data set.

591 The first principal component (PC1) contains information primarily about rare earth elements. The
592 correlation of each element with PC1 is as follows: Ce(0.982), La(0.979), Pr(0.992), Nd (0.994), Sm(0.995),
593 and Eu (0.789).

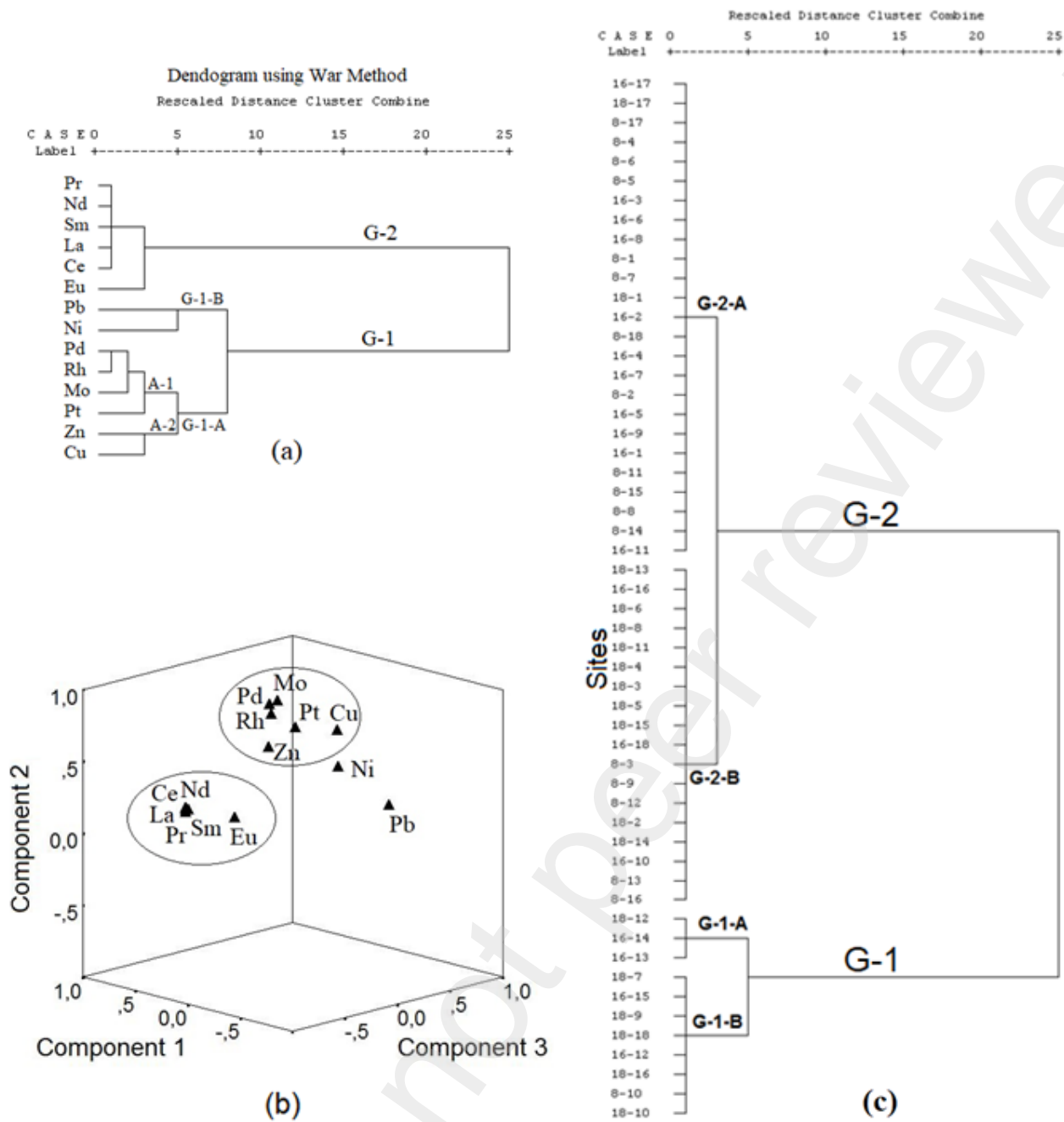
594 The second principal component (PC2) encompasses information mainly about PGEs - Mo, Cu, and
595 Zn. Below, are the correlations of these elements with PC2: Pd(0.896), Pt(0.765), Rh(0.930), Mo(0.833),
596 Cu(0.673), Zn(0.609), and Ni(0.306).

597 The third principal component (PC3) solely contains information about Pb(0.787) and Ni(0.612),
598 isolating them from the other two groups.

599 Positioning the variables in a three-dimensional space, as shown in Fig. 5b, reveals that Pd, Pt, Rh,
600 Mo, Zn, and Cu are separated by PC2 from another group composed of rare earth elements (Ce, La, Nd, Pr,
601 and Eu) with similar behavior. Additionally, Pb and Ni are separated by PC3 from the groups formed by
602 elements showing contamination due to the growth of the vehicle fleet and from the other group of rare earth
603 elements originated from natural weathering processes.

604 Figure 5c illustrates the groups characterized by the average values and standard deviations of each
605 analyzed PGE. Group G1, comprising 11 samples, displayed significantly higher average concentrations of
606 Pd, Pt, and Rh compared to Group G2, which consisted of 32 samples. Specifically, the concentrations of
607 Pd, Pt, and Rh in G1 were found to be 4.2, 2.2, and 3.3 times higher, respectively, than those observed in
608 G2. These findings indicate that G1 corresponds to sites with a critical level of PGE contamination, while
609 G2 represents road dust samples with lower levels of PGEs.

610



611 **Figure 5.** Dendrogram from the cluster analysis for PGEs, Mo, Pb, Ni, Cu, Zn and rare earths (a), PCA for
 612 the elements (b) and PGEs concentrations in road dust samples collected from São Paulo (c).
 613
 614

615 The group G-1 was divided into two other closely similar groups. G1-A comprised three samples
 616 from Rebouças Avenue (P12-2018), Paulista Avenue (P14-2016), and Consolação Avenue (P13-2016),
 617 which showed the highest concentrations of PGEs. The average concentrations of Pd, Pt, and Rh in G1-A
 618 were respectively 1.7, 1.6, and 1.9 times higher than those elements in Group-1-B. Group 2 was also divided
 619 into two highly similar subgroups based on the concentration of PGEs in the samples. Group-2-B, consisting
 620 of 18 samples, exhibited mean concentrations of Pd, Pt, and Rh that were 2.8, 1.1, and 2.2 times higher,
 621 respectively, than those elements in Group-2-A, which included 25 samples. At the top of Fig. 5c are

622 displayed the samples with the lowest concentrations of PGEs, namely P17-2008, P17-2016, and P17-2018,
623 collected from road dust samples in low traffic volume local pavements (Ipen-Parking).

624 **4. Conclusions**

625 PGEs levels in road dust samples collected from the city of São Paulo in 2008, 2016, and 2018
626 showed a significant increase over the ten-year period. The median concentration of Palladium (Pd)
627 increased by 139%, Rhodium (Rh) increased by 87%, while Platinum (Pt) decreased by 19%.

628 The PGEs increase was supported by the metal pollution index (MPI) mean, which varied from 90 in
629 2008 to 123 in 2016 and 143 in 2018. Locations with the highest MPI values during all collections were
630 streets or avenues with speed limits of 40 or 50 km/hour, traffic lights, and frequent stop-and-go traffic,
631 leading to increased fuel burning.

632 Enrichment factors (EF) also supported the rise in PGEs levels over this 10-year period, with EF
633 values compared to Samarium's (Sm) crustal abundance exceeding 40, indicating extremely high
634 enrichment. Specifically, EF values for Pd and Rh increased between 2008, 2016, and 2018: Pd EF values of
635 509, 942, and 1507, and Rh EF values of 487, 729, and 1119, respectively. In contrast, Pt EF values were
636 lower, measuring 142, 128, and 148 for the corresponding years. These increases align with the growing
637 number of vehicles equipped with catalytic converters in São Paulo city, suggesting vehicular sources
638 contribute to the presence of PGEs in the collected road dust samples.

639 PGEs, Mo, Zn, and Cu EF exhibited an increase in road dust samples from 2008 to 2018, showing
640 strong correlations among themselves. This supports the hypothesis that PGEs, Mo, Cu, and Zn in the São
641 Paulo environment likely originate from the same source, namely automotive emissions. On the other hand,
642 the other elements did not show an increase in EF during this 10-year period. Although Pb and Ni presented
643 some sites with significant enrichment, these sites were not the same as those most impacted by very high
644 enrichment and extremely high enrichment observed for the PGEs. Therefore, Pb and Ni enrichment seem to
645 be of non-vehicular origins. The rare earth elements in road dust samples predominantly originated from the
646 natural erosion of crustal material.

647 The presence of PGEs in road dust samples, with potential health risks, is little known. Long-term
648 vehicle catalyst use may lead to PGEs bioaccumulation in urban areas. While converters reduce toxic

emissions, they add to pollution. São Paulo's high vehicle numbers impact human health and the urban environment, necessitating mobility and pollution reduction policies. Limited mobility and traffic hinder engine efficiency and emission reduction progress. Electric and hydrogen cars control pollution without PGE-containing converters, but the environmental impact of electric car batteries, as well as the origin of the energy that supplies the batteries, must be considered. Policies promoting zero-emission electric public transport can enhance urban mobility. This study provides PGEs concentration data from São Paulo, enabling pollution monitoring in future research.

Acknowledgments

The authors thanks to the Ipen/CNEN-SP for their support in this study.

Appendix A. Supplementary data

Supplementary data to this article can be found online at <https://doi.org/>

References

- Alsenz, H., Zereini, F., Wiseman, C. L. S., & Puttmann, W. (2009). Analysis of palladium concentrations in airborne particulate matter with reductive co-precipitation, He collision gas, and ID-ICP-Q-MS. *Analytical and Bioanalytical Chemistry*, 395(6), 1919-1927. <https://doi.org/10.1007/s00216-009-3143-8>
- Baldanza, M. A. S., de Mello, L. F., Vannice, A., Noronha, F. B., & Schmal, M. (2000). Adsorptive and catalytic properties of alumina-supported Pd-Mo catalysts. *Journal of Catalysis*, 192(1), 64-76. <https://doi.org/10.1006/jcat.2000.2839>
- Barbante, C., Veyseyre, A., Ferrari, C., Van de Velde, K., Morel, C., Capodaglio, G., . . . Boutron, C. (2001). Greenland snow evidence of large scale atmospheric contamination for platinum, palladium, and rhodium. *Environmental Science & Technology*, 35(5), 835-839. <https://doi.org/10.1021/es000146y>
- Birke, M., Rauch, U., Stummeyer, J., Lorenz, H., & Keilert, B. (2018). A review of platinum group element (PGE) geochemistry and a study of the changes of PGE contents in the topsoil of Berlin, Germany, between 1992 and 2013. *Journal of Geochemical Exploration*, 187, 72-96. <https://doi.org/10.1016/j.gexplo.2017.09.005>
- Buatmenard, P., & Chesselet, R. (1979). VARIABLE INFLUENCE OF THE ATMOSPHERIC FLUX ON THE TRACE-METAL CHEMISTRY OF OCEANIC SUSPENDED MATTER. *Earth and Planetary Science Letters*, 42(3), 399-411. [https://doi.org/10.1016/0012-821x\(79\)90049-9](https://doi.org/10.1016/0012-821x(79)90049-9)
- da Silva, Y., do Nascimento, C. W. A., Biondi, C. M., & Silva, C. (2016). Rare Earth Element Concentrations in Brazilian Benchmark Soils. *Revista Brasileira De Ciencia Do Solo*, 40, Article e0150413. <https://doi.org/10.1590/18069657rbcS20150413>
- CETESB , EMISSÕES VEICULARES NO ESTADO DE SÃO PAULO 2019, Série relatórios - São Paulo/SP – 2020. <https://cetesb.sp.gov.br/veicular/wp-content/uploads/sites/6/2020/11/Relatorio-Emissoes-Veiculares-no-Estado-de-Sao-Paulo-2019.pdf>
- Ellison, S. L. R., Rosslein, M., & Williams, A. (2002). Determinando a incerteza na medição analítica. Guide EURACHEM/CITAC. 2ª ed

- 688 Ferreira-Baptista, L., & De Miguel, E. (2005). Geochemistry and risk assessment of street dust in Luanda,
689 Angola: A tropical urban environment. *Atmospheric Environment*, 39(25), 4501-4512.
690 <https://doi.org/10.1016/j.atmosenv.2005.03.026>
- 691 Gao, B., Yu, Y. K., Zhou, H. D., & Lu, J. (2012). Accumulation and distribution characteristics of platinum
692 group elements in roadside dusts in Beijing, China. *Environmental Toxicology and Chemistry*, 31(6),
693 1231-1238. <https://doi.org/10.1002/etc.1833>
- 694 Gomez, M. B., Gomez, M. M., & Palacios, M. A. (2000). Control of interferences in the determination of Pt,
695 Pd and Rh in airborne particulate matter by inductively coupled plasma mass spectrometry. *Analytica
696 Chimica Acta*, 404(2), 285-294. [https://doi.org/10.1016/s0003-2670\(99\)00723-0](https://doi.org/10.1016/s0003-2670(99)00723-0)
- 697 Gomez, M. B., Gomez, M. M., & Palacios, M. A. (2003). ICP-MS determination of Pt, Pd and Rh in
698 airborne and road dust after tellurium coprecipitation. *Journal of Analytical Atomic Spectrometry*,
699 18(1), 80-83. <https://doi.org/10.1039/b209727n>
- 700 Hann, S., Koellensperger, G., Kanitsar, K., & Stingeder, G. (2001). ICP-SFMS determination of palladium
701 using IDMS in combination with on-line and off-line matrix separation. *Journal of Analytical Atomic
702 Spectrometry*, 16(9), 1057-1063. <https://doi.org/10.1039/b102574k>
- 703 Hortellani, M. A., Sarkis, J. E. S., Menezes, L. C. B., Bazante-Yamaguishi, R., Pereira, A. S. A., Garcia, P.
704 F. G., . . . Genova de Castro, P. M. (2013). Assessment of Metal Concentration in the Billings
705 Reservoir Sediments, Sao Paulo State, Southeastern Brazil. *Journal of the Brazilian Chemical
706 Society*, 24(1), 58-67. <https://doi.org/10.1590/S0103-50532013000100009>
- 707 Hsu, W. H., Jiang, S. J., & Sahayam, A. C. (2013). Determination of Pd, Rh, Pt, Au in road dust by
708 electrothermal vaporization inductively coupled plasma mass spectrometry with slurry sampling.
709 *Analytica Chimica Acta*, 794, 15-19. <https://doi.org/10.1016/j.aca.2013.08.001>
- 710 IBGE, Population São Paulo city in 2023. <https://cidades.ibge.gov.br/brasil/sp/sao-paulo/panorama>
711 IBGE, Cities-Brazil (*Vehicles fleet*). [https://cidades.ibge.gov.br/brasil/sp/sao-
712 paulo/pesquisa/22/28120?ano=2018](https://cidades.ibge.gov.br/brasil/sp/sao-paulo/pesquisa/22/28120?ano=2018)
- 713 INMETRO-National Institute of Metrology, Quality and Technology (2019) Orientação sobre validação de
714 métodos analíticos [http://www.inmetro.gov.br/Sidoq/
715 Arquivos/Cgcre/DOQ/DOQ-Cgcre-8_04.pdf](http://www.inmetro.gov.br/Sidoq/Arquivos/Cgcre/DOQ/DOQ-Cgcre-8_04.pdf)
- 716 Jarvis, K. E., Parry, S. J., & Piper, J. M. (2001). Temporal and spatial studies of autocatalyst-derived
717 platinum, rhodium. and palladium and selected vehicle derived trace elements in the environment.
718 *Environmental Science & Technology*, 35(6), 1031-1036. <https://doi.org/10.1021/es0001512>
- 719 Kalavrouziotis, I. K., & Koukoulakis, P. H. (2009). The Environmental Impact of the Platinum Group
720 Elements (Pt, Pd, Rh) Emitted by the Automobile Catalyst Converters. *Water Air and Soil Pollution*,
721 196(1-4), 393-402. <https://doi.org/10.1007/s11270-008-9786-9>
- 722 Kanitsar, K., Koellensperger, G., Hann, S., Limbeck, A., Puxbaum, H., & Stingeder, G. (2003).
723 Determination of Pt, Pd and Rh by inductively coupled plasma sector field mass spectrometry (ICP-
724 SFMS) in size-classified urban aerosol samples. *Journal of Analytical Atomic Spectrometry*, 18(3),
725 239-246. <https://doi.org/10.1039/b212218a>
- 726 Klaminder, J., Bindler, R., Emteryd, O., Appleby, P., & Grip, H. (2006). Estimating the mean residence time
727 of lead in the organic horizon of boreal forest soils using 210-lead, stable lead and a soil
728 chronosequence. *Biogeochemistry*, 78(1), 31-49. <https://doi.org/10.1007/s10533-005-2230-y>
- 729 Kovacheva, P., & Djingova, R. (2002). Ion-exchange method for separation and concentration of platinum
730 and palladium for analysis of environmental samples by inductively coupled plasma atomic emission
731 spectrometry. *Analytica Chimica Acta*, 464(1), 7-13, Article Pii s0003-2670(02)00428-2.
732 [https://doi.org/10.1016/s0003-2670\(02\)00428-2](https://doi.org/10.1016/s0003-2670(02)00428-2)
- 733 Lesniewska, B. A., Godlewska-Zylkiewicz, B., Ruszczynska, A., Bulska, E., & Hulanicki, A. (2006).
734 Elimination of interferences in determination of platinum and palladium in environmental samples
735 by inductively coupled plasma mass spectrometry. *Analytica Chimica Acta*, 564(2), 236-242.
736 <https://doi.org/10.1016/j.aca.2006.01.066>
- 737 Lima, L. H. V., do Nascimento, C. W. A., da Silva, F. B. V., & Araujo, P. R. M. (2023). Baseline
738 concentrations, source apportionment, and probabilistic risk assessment of heavy metals in urban
739 street dust in Northeast Brazil. *Science of the Total Environment*, 858, Article 159750.
<https://doi.org/10.1016/j.scitotenv.2022.159750>

- 740 Magnusson, B., Krysell, M., Sahlin, E., & Näykki, T. (2020). Uncertainty from sampling, Nordest Report
741 TR 604 (2nd). Available from www.nordtest.info
- 742 Merget, R., & Rosner, G. (2001). Evaluation of the health risk of platinum group metals emitted from
743 automotive catalytic converters. *Science of the Total Environment*, 270(1-3), 165-173.
744 [https://doi.org/10.1016/s0048-9697\(00\)00788-9](https://doi.org/10.1016/s0048-9697(00)00788-9)
- 745 Miguel A.H. and de Andrade J.B. (1990). Catalyst and Noncatalyst Exhaust Aldehydes Emissions from
746 Brazilian Ethanol-Fueled Vehicles. *Journal of the Brazilian Chemical Society*, 1(3), 124-128.
747 <https://doi.org/10.1590/S0103-50532013000100009>
- 748 Moldovan, M., Gomez, M. M., & Palacios, M. A. (1999). Determination of platinum, rhodium and
749 palladium in car exhaust fumes. *Journal of Analytical Atomic Spectrometry*, 14(8), 1163-1169.
750 <https://doi.org/10.1039/a901516g>
- 751 Moldovan, M., Rauch, S., Gomez, M., Palacios, M. A., & Morrison, G. M. (2001). Bioaccumulation of
752 palladium, platinum and rhodium from urban particulates and sediments by the freshwater isopod
753 *Asellus aquaticus*. *Water Research*, 35(17), 4175-4183. [https://doi.org/10.1016/s0043-1354\(01\)00136-1](https://doi.org/10.1016/s0043-1354(01)00136-1)
- 754
- 755 Morcelli, C. P. R., Figueiredo, A. M. G., Sarkis, J. E. S., Enzweiler, J., Kakazu, M., & Sigolo, J. B. (2005).
756 PGEs and other traffic-related elements in roadside soils from Sao Paulo, Brazil. *Science of the Total
757 Environment*, 345(1-3), 81-91. <https://doi.org/10.1016/j.scitotenv.2004.10.018>
- 758 Motelica-Heino, M., Rauch, S., Morrison, G. M., & Donard, O. F. X. (2001). Determination of palladium,
759 platinum and rhodium concentrations in urban road sediments by laser ablation-ICP-MS. *Analytica
760 Chimica Acta*, 436(2), 233-244. [https://doi.org/10.1016/s0003-2670\(01\)00967-9](https://doi.org/10.1016/s0003-2670(01)00967-9)
- 761 Nory, R. M., Figueiredo, A. M. G., Souto-Oliveira, C. E., & Babinski, M. (2021). Urban contamination
762 sources in tunnel dusts from Sa similar to o Paulo city: Elemental and isotopic characterization.
763 *Atmospheric Environment*, 254, Article 118188. <https://doi.org/10.1016/j.atmosenv.2021.118188>
- 764 Okafor, E. C., & Opuene, K. (2007). Preliminary assessment of trace metals and polycyclic aromatic
765 hydrocarbons in the sediments. *International Journal of Environmental Science and Technology*,
766 4(2), 233-240. <https://doi.org/10.1007/bf03326279>
- 767 Okorie, I. A., Enwistle, J., & Dean, J. R. (2015). Platinum group elements in urban road dust. *Current
768 Science*, 109(5), 938-942. <https://doi.org/10.18520/v109/i5/938-942>
- 769 Qi, L., Zhou, M. F., Zhao, Z., Hu, J., & Huang, Y. (2011). The characteristics of automobile catalyst-derived
770 platinum group elements in road dusts and roadside soils: a case study in the Pearl River Delta
771 region, South China. *Environmental Earth Sciences*, 64(6), 1683-1692.
772 <https://doi.org/10.1007/s12665-010-0635-y>
- 773 Ramsey, M. H., Ellison, S. L. R. (2007). Measurement uncertainty arising from sampling: A guide to
774 methods and approaches. Eurachem EUROLAB CITAC Nordtest and the RSC Analytical Methods
775 Committee 1rst Ed
- 776 Ravindra, K., Bencs, L., & Van Grieken, R. (2004). Platinum group elements in the environment and their
777 health risk. *Science of the Total Environment*, 318(1-3), 1-43. [https://doi.org/10.1016/s0048-9697\(03\)00372-3](https://doi.org/10.1016/s0048-9697(03)00372-3)
- 778
- 779 Ribeiro, A. P., Figueiredo, A. M. G., Sarkis, J. E. S., Hortellani, M. A., & Markert, B. (2012). First study on
780 anthropogenic Pt, Pd, and Rh levels in soils from major avenues of So Paulo City, Brazil.
781 *Environmental Monitoring and Assessment*, 184(12), 7373-7382. <https://doi.org/10.1007/s10661-011-2506-8>
- 782
- 783 Spada, N., Bozlaker, A., & Chellam, S. (2012). Multi-elemental characterization of tunnel and road dusts in
784 Houston, Texas using dynamic reaction cell-quadrupole-inductively coupled plasma-mass
785 spectrometry: Evidence for the release of platinum group and anthropogenic metals from motor
786 vehicles. *Analytica Chimica Acta*, 735, 1-8. <https://doi.org/10.1016/j.aca.2012.05.026>
- 787 Sutherland, R. A. (2000). Bed sediment-associated trace metals in an urban stream, Oahu, Hawaii.
788 *Environmental Geology*, 39(6), 611-627. <https://doi.org/10.1007/s002540050473>
- 789 Sutherland, R. A. (2007). Platinum-group element concentrations in BCR-723: A quantitative review of
790 published analyses. *Analytica Chimica Acta*, 582(2), 201-207.
791 <https://doi.org/10.1016/j.aca.2006.09.030>

- 792 Sutherland, R. A., Pearson, D. G., & Ottley, C. J. (2008). Grain size partitioning of platinum-group elements
793 in road-deposited sediments: Implications for anthropogenic flux estimates from autocatalysts.
794 *Environmental Pollution*, 151(3), 503-515. <https://doi.org/10.1016/j.envpol.2007.04.018>
- 795 Tessari-Zampieri, M. C., Sarkis, J. E. S., & Barbieri, C. B. (2022). Metrological Aspects of Platinum Group
796 Elements Atmospheric Deposition in Roadside Tree Leaves: Uncertainties and Environmental Data
797 Interpretation. *Water Air and Soil Pollution*, 233(3), Article 91. <https://doi.org/10.1007/s11270-022-05549-1>
- 798
- 799 Usero, J., GonzalezRegalado, E., & Gracia, I. (1996). Trace metals in the bivalve mollusc *Chamelea gallina*
800 from the Atlantic coast of southern Spain. *Marine Pollution Bulletin*, 32(3), 305-310.
801 [https://doi.org/10.1016/0025-326x\(95\)00209-6](https://doi.org/10.1016/0025-326x(95)00209-6)
- 802 Verstraete, D., Riondato, J., Vercauteren, J., Vanhaecke, F., Moens, L., Dams, R., & Verloo, M. (1998).
803 Determination of the uptake of Pt(NH₃)(4) (NO₃)(2) by grass cultivated on a sandy loam soil and by
804 cucumber plants, grown hydroponically. *Science of the Total Environment*, 218(2-3), 153-160.
805 [https://doi.org/10.1016/s0048-9697\(98\)00204-6](https://doi.org/10.1016/s0048-9697(98)00204-6)
- 806 Wedepohl, K. H. (1995). THE COMPOSITION OF THE CONTINENTAL-CRUST. *Geochimica Et*
807 *Cosmochimica Acta*, 59(7), 1217-1232.
- 808 Whiteley, J. D. (2005). Seasonal variability of platinum, palladium and rhodium (PGE) levels in road dusts
809 and roadside soils, perth, Western Australia. *Water Air and Soil Pollution*, 160(1-4), 77-93.
810 <https://doi.org/10.1007/s11270-005-3861-2>
- 811 Whiteley, J. D., & Murray, F. (2003). Anthropogenic platinum group element (Pt, Pd and Rh) concentrations
812 in road dusts and roadside soils from Perth, Western Australia. *Science of the Total Environment*,
813 317(1-3), 121-135. [https://doi.org/10.1016/s0048-9697\(03\)00359-0](https://doi.org/10.1016/s0048-9697(03)00359-0)
- 814 Whiteley, J. D., & Murray, F. (2005). Autocatalyst-derived platinum, palladium and rhodium (PGE) in
815 infiltration basin and wetland sediments receiving urban runoff. *Science of the Total Environment*,
816 341(1-3), 199-209. <https://doi.org/10.1016/j.scitotenv.2004.09.030>
- 817 Wichmann, H., Anquandah, G. A. K., Schmidt, C., Zachmann, D., & Bahadir, M. A. (2007). Increase of
818 platinum group element concentrations in soils and airborne dust in an urban area in Germany.
819 *Science of the Total Environment*, 388(1-3), 121-127. <https://doi.org/10.1016/j.scitotenv.2007.07.064>
- 820 Wiseman, C. L. S., Niu, J. J., Levesque, C., Chenier, M., & Rasmussen, P. E. (2018). An assessment of the
821 inhalation bioaccessibility of platinum group elements in road dust using a simulated lung fluid.
822 *Environmental Pollution*, 241, 1009-1017. <https://doi.org/10.1016/j.envpol.2018.06.043>
- 823 Zhong, L. F., Li, J., Yan, W., Tu, X. L., Huang, W. X., & Zhang, X. H. (2012). Platinum-group and other
824 traffic-related heavy metal contamination in road sediment, Guangzhou, China. *Journal of Soils and*
825 *Sediments*, 12(6), 942-951. <https://doi.org/10.1007/s11368-012-0527-8>
- 826 Zimmermann, S., Wolff, C., & Sures, B. (2017). Toxicity of platinum, palladium and rhodium to *Daphnia*
827 *magna* in single and binary metal exposure experiments. *Environmental Pollution*, 224, 368-376.
828 <https://doi.org/10.1016/j.envpol.2017.02.016>